Entirely Aqueous Solution−Gel Route for the Preparation of $(Pb_{1-x}Ca_x)TiO_3$ Thin Films

I. Bretos,[†,*] R. Jiménez,[†] M. L. Calzada,[†] M. K. Van Bael,[‡] A. Hardy,[‡] D. Van Genechten,[‡] and J. Mullens[‡]

Instituto de Ciencia de Materiales de Madrid, CSIC, Cantoblanco 28049 Madrid, Spain, and Hasselt University and IMEC vzw, Division IMOMEC, Inorganic and Physical Chemistry group, Agoralaan building D, B-3590 Diepenbeek, Belgium

Received July 28, 2006. Revised Manuscript Received October 3, 2006

In this work, calcium-modified lead titanate $(Pb_{1-x}Ca_x)TiO_3$ (PCT) precursor solutions with different amounts of Ca^{2+} substituting Pb^{2+} ($x = 0.24$ and 0.50) have been prepared for the first time by an entirely aqueous solution−gel route. The use of water as a nonhazardous and inexpensive solvent, together with the easy handling of the technique (no inert atmosphere is required), are the major advantages of this method. A stable citrato-peroxo complex of Ti(IV) was synthesized first and subsequently combined with the Pb^{2+} and Ca^{2+} reagents (citrates) in the desired molar ratio to obtain the aqueous precursor solutions. The stability of these solutions with time is slightly influenced by the amount of Ca^{2+} introduced in the PCT system. Gels were obtained from these solutions and subjected to thermogravimetric analysis coupled on-line to Fourier transform infrared (TGA−FTIR) and mass spectroscopy (TGA−MS) techniques. To prepare thin films, we had to improve the hydrophilicity of the $Pt/TiO_x/SiO_2/Si$ substrates and hence their wetting by the aqueous solutions using a wet chemical treatment of cleaning. Crystallization of the films was carried out by rapid thermal processing (RTP) in air at 650 °C. Films with a single perovskite phase and a homogeneous microstructure were thus obtained, as deduced by X-ray diffraction (XRD) and scanning electron microscopy (SEM). The ability of this solution method to obtain PCT films with ferroelectric and dielectric responses is also demonstrated in the present work.

1. Introduction

Ferroelectric compositions based on the lead titanate perovskite, $PbTiO_3$ (PT), day after day continue generating a great deal of research in both bulk ceramic and thin film forms because of their potential applications in functional electronic devices. The partial substitution of Pb^{2+} by Ca^{2+} at the A site of the perovskite leads to calcium-modified lead titanate, $(Pb_{1-x}Ca_x)TiO_3$ (PCT), which presents different properties as a function of the degree of substitution introduced into the system.[1] Compositions of PCT with Ca^{2+} contents below 35 at. % ($x < 0.35$) in thin film form have been extensively studied because of their ferro-, pyro-, and piezoelectric responses,[2] which are of interest in nonvolatile ferroelectric random access memories (NVFeRAMs), infrared sensors or microelectromechanical systems (MEMs), respectively. Furthermore, PCT films with larger amounts of Pb^{2+} substituted by Ca^{2+} ($x \geq 0.40$) have recently been shown to possess relaxorlike character,[3] with a diffuse ferroparaelectric transition, high values of permittivity at room temperature, and a large nonlinearity of this value with the applied bias field. These are characteristics that can be exploited in dynamic random access memories (DRAMs) for charge storage and voltage-tunable devices (e.g., varactors).[4]

However, the fabrication of high-performance ceramic materials usually involves environmental and economical costs related to the use of hazardous substances, energy consumption, and waste generation during the whole process. In the case of the electronic industry, environmental awareness is demanded ever more,[5] restricting particularly the use of lead in electrical and electronic equipment, although lead in electronic ceramic parts is exempt from these restrictions at the moment. As long as a viable lead-free replacement is not fully developed and compositions based on lead (mainly represented by $Pb(Zr,Ti)O_3$ and $PbTiO_3$) remain the most important alternatives in the fabrication of dielectric, ferroelectric, or piezoelectric materials,[6] the environmentally friendly trend must also target the development of low-toxicity processes (low-toxicity solvents and reagents, low thermal budgets, etc.).

* Corresponding author. E-mail: ibretos@icmm.csic.es.
† Instituto de Cienca de Materials de Madrid, CSIC.
‡ Hasselt University and IMEC vzw.

(1) Mendiola, J.; Jiménez, B.; Alemany, C.; Pardo, L.; del Olmo, L. *Ferroelectrics* **1989**, *94*, 183.
(2) Mendiola, J.; Calzada, M. L. Ferroelectric Thin Films of Modified Lead Titanate. In *Handbook of Thin Film Materials*; Nalwa, H., Ed.; Academic Press: London, 2002; Vol. 3, Chapter 6, p 369.
(3) Jiménez, R.; Alemany, C.; Calzada, M. L.; Mendiola, J. *Ferroelectrics* **2004**, *302*, 461.
(4) Mendiola, J.; Jiménez, R.; Ramos, P.; Alemany, C.; Bretos, I.; Calzada, M. L. *J. Appl. Phys.* **2005**, *98* (2), 024106.
(5) *Directive 2002/95/EC of the European Parliamentand of the Council on the Restriction Of the Use of Certain Hazardous Substances in Electrical and Electronic Equipment*, Brussels, Belgium, Jan 27, 2003.
(6) Gonnard, P.; Simon-Seveyrat, L. Environmentally Conscious Electroceramics. In *Processing of Electroceramics*, Proceedings of the POLECER Symposium on Processing of Electroceramics, Bled, Slovenia, Aug 31−Sept 3, 2003; Kosec, M., Kuscer, D., Malic, B., Eds.; Institute Jozef Stefan: Ljubljana, Slovenia, 2003; p 331.

10.1021/cm061767e CCC: $33.50
Published on Web 12/01/2006

For the synthesis of such ceramic materials, chemical solution deposition (CSD)[7] methods are low-energy processes compared to solid- and/or vapor-state reactions, which is one of the key advantages of soft solution processing of advanced materials.[8] However, one of the major problems concerning most CSD methods is the toxicity of the solvents and reagents normally used in the laboratory. The majority of the works reporting about chemical solution preparation of multimetal precursors[9−11] use organic solvents that are recognized as highly toxic (carcinogens (benzene), reproductive hazards (2-methoxyethanol, 2-ethoxyethanol), neurotoxins (toluene, *n*-hexane), or depressants of the central nervous system (xylene, buthoxyethanol)), and therefore involve health risks in addition to the environmental impact they might have. Other handicaps, such as, for example, the hydrolysis sensitivity of the alkoxides used as starting reagents, add technological problems to the fabrication process. Both ecological and/or technical aspects hamper the application of these processes in the industrial sector and necessitate the search for alternative processing routes for the fabrication of dielectric and ferroelectric ceramic thin films.

An entirely aqueous synthetic route would solve the aforementioned problems, because water is used instead of organic solvents, promoting ecological benefits and even reducing the costs associated with the technique (chemicals and equipment). However, to the best of the authors' knowledge, few works report on the successful preparation of multimetal dielectric and ferroelectric thin films by an entirely aqueous solution method.[12,13] Films of (Pb,La)(Zr,Ti)O_3 (PLZT) and Pb(Zr,Ti)O_3 (PZT) compositions have been prepared by an alternative MOD process, using the deposition by aqueous acetate solution (DAAS) technique.[14,15] However, to obtain crackfree films or improve surface wetting adhesion, one must add alcohols such as methanol[14] or polyvinyl alcohol (PVA)/glycerol[15] to the respective aqueous precursor solutions prior to film deposition. Also, in the Pechini process,[16] despite an alpha hydroxycarboxylic acid (citric acid) being used instead of any organic solvent to chelate with the cation precursors, a polyhydroxy alcohol (ethylene glycol) must be subsequently added to promote polyesterification and formation of a spineable sol network after heating. Therefore, although multimetal oxide precursors can be obtained by aqueous solution methods,[14−19] the preparation of high-quality films from these solutions turns into a difficult task that requires the enhancement of the solution rheology by the addition of organic solvents, normally alcohols.

Until now, the synthesis of the PCT perovskite composition by an entirely aqueous solution method has not been attempted. Precursor solutions of PCT with Ca^{2+} contents less than 40 at. % ($x \leq 0.40$) have been synthesized using organic solvents such as methoxyethanol,[20] methanol,[21,22] ethylene glycol,[23] or 1,3-propanediol[24−26]. For Ca^{2+} contents greater 40 at. %, only some of the authors of this work have tested the preparation of $(Pb_{0.50}Ca_{0.50})TiO_3$ ($x = 0.50$) solutions using a diol-based sol−gel route.[27] The low solubility that the calcium compounds exhibit in the organic solvents normally used is one of the major problems found in the synthesis of precipitate-free solutions of PCT, mainly when Ca^{2+} contents over 40 at. % are used.[28]

In this work, the development of an entirely aqueous solution−gel method for the synthesis of precursor solutions of $(Pb_{1-x}Ca_x)TiO_3$, with $0 \leq x \leq 0.50$, is presented for the first time. This aqueous solution−gel process is based on the use of water instead of any organic solvent, and coordinating ligands such as citrates and peroxides.[29,30] These chelating agents show the ability to coordinate the different metal cations present in the solution, hence preventing their solvatation by the water molecules that would lead to the uncontrolled hydrolysis and subsequent precipitation of the hydroxides/oxides formed.[31] The reliability of this aqueous solution method has been previously proved in other multimetal oxide compositions such as PZT, $SrBi_2Ta_2O_9$ (SBT), and $(Bi_{1-x}La_x)_4Ti_3O_{12}$ (BLT), among others. The feasibility of this process obtaining PCT crystalline films with ferroelectric and dielectric responses will be also discussed. The importance of this aqueous solution−gel method as an interesting approach to minimizing the amount of toxic chemicals during solution processing is therefore addressed.

2. Experimental Section

2.1. Solutions and Gels. Aqueous precursor solutions of PCT were obtained by the route shown in the schematic diagram of Figure 1. First, a stable aqueous Ti(IV) precursor was synthesized

(7) Schwartz R. W.; Schneller T.; Waser R. *C. R. Chimie* **2004**, *7*, 433.
(8) Yoshimura, M. *J. Mater. Res.* **1998**, *13* (4), 796.
(9) Dekleva, T. W.; Hayes, J. M.; Cross, L. E.; Geoffroy, G. L. *J. Am. Ceram. Soc.* **1988**, *7* (5), C-280.
(10) Zai, M. H. M.; Akiba, A.; Goto, H.; Matsumoto, M.; Yeatman, E. M. *Thin Solid Films* **2001**, *394* (1−2), 97.
(11) Suyama, Y.; Noritake, T.; Nagasawa, M. *Jpn. J. Appl. Phys., Part 1* **1997**, *36* (9B), 5939.
(12) Van Bael, M. K.; Nelis, D.; Hardy, A.; Mondelaers, D.; Van Werde, K.; D'Haen, J.; Vanhoyland, G.; Van Den Rul, H.; Mullens, J.; Van Poucke, L. C.; Frederix, F.; Wouters, D. J. *Integr. Ferroelectr.* **2002**, *45*, 113.
(13) Hardy, A.; Nelis, D.; Vanhoyland, G.; Van Bael, M. K.; Mullens, J.; Van Poucke, L. C.; D'Haen, J.; Wouters, D. J. *Integr. Ferroelectr.* **2004**, *62*, 205.
(14) Haertling, G. *Ferroelectrics* **1991**, *116*, 51.
(15) Lin, C. T.; Li, L.; Webb, J. S.; Russell, A.; Lipeles, R. A.; Leung, M. S. *Integr. Ferroelectr.* **1993**, *3*, 333.
(16) Pechini, M. P. U.S. Patent 3 330 697, 1967.
(17) Lee, B.; Zhang, J. *Thin Solid Films* **2001**, *388*, 107.
(18) Asai, T.; Camargo, E. R.; Kakihana, M.; Osada, M. *J. Alloys Compd.* **2000**, *309*, 113.
(19) Schäfer, J.; Sigmund, W.; Roy, S.; Aldinger, F. *J. Mater. Res.* **1997**, *12* (10), 2518.
(20) Chopra, S., Sharma, S., Goel, T. C.; Mendiratta, R. G. *Appl. Surf. Sci.* **2004**, *230*, 207.
(21) Li, H.; Tang, X.; Li, Q.; Liu, Y.; Tang, Z.; Zhang, Y.; Mo, D. *Solid State Commun.* **2000**, *114*, 347.
(22) Bao, D.; Wu, X.; Zhang, L.; Yao, X. *Thin Solid Films* **1999**, *350*, 30.
(23) Pontes, D. S. L.; Leite, E. R.; Pontes, F. M.; Longo, E.; Varela, J. A. *J. Eur. Ceram. Soc.* **2001**, *21*, 1107.
(24) Sirera, R.; Calzada, M. L. *Mater. Res. Bull.* **1995**, *30* (1), 11.
(25) Wang, C. M.; Huang, Y. T.; Chen, Y. C.; Lee, M. S.; Kao, M. C. *Jpn. J. Appl. Phys.* **2000**, *39*, 3579.
(26) Chewasatn, S.; Milne, S. J. *J. Mater. Sci.* **1997**, *32* (3), 575.
(27) Bretos, I.; Ricote, J.; Jiménez, R.; Mendiola, J.; Calzada, M. L. *Integr. Ferroelectr.* **2004**, *61*, 105.
(28) Calzada, M. L.; Bretos, I.; Jiménez, R.; Ricote, J.; Mendiola, J.; García-López, J.; Respaldiza, M. A. *J. Am. Ceram. Soc.* **2005**, *88* (12), 3388.
(29) Van Bael, M. K.; Arcon, I.; Van Werde, K.; Nelis, D.; Mullens, J.; Van Poucke, L. C. *Phys. Scr.* **2005**, *T115*, 415.
(30) Narendar, Y.; Messing, G. L. *Chem. Mater.* **1997**, *9*, 580.
(31) Livage, J.; Henry, M.; Sanchez, C. *Prog. Solid. State Chem.* **1988**, *18*, 259.

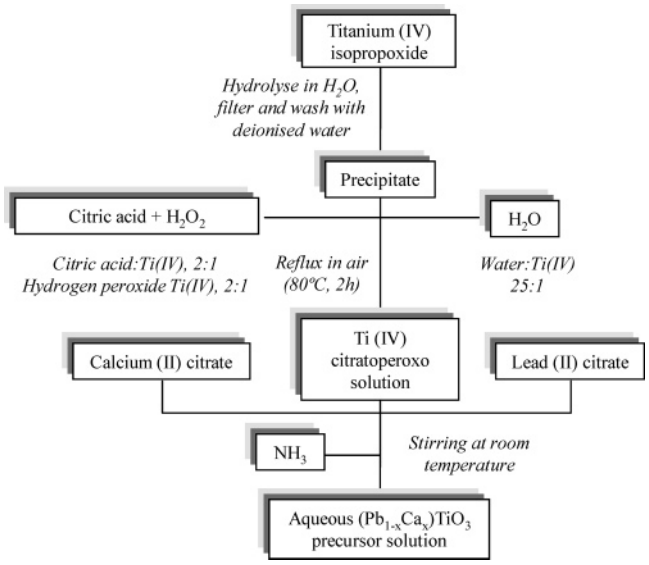

Figure 1. Schematic diagram of the aqueous solution−gel synthetic route.

according to the procedure described in ref 32. Titanium (IV) tetraisopropoxide ($Ti(OCH(CH_3)_2)_4$, Acros Organics, 98+%) was hydrolyzed in water, leading to the formation of a precipitate (titanium hydroxide) that was filtered and washed with deionized water. Citric acid ($HOOCCH_2C(OH)(COOH)CH_2COOH$, Aldrich, 99%), hydrogen peroxide (H_2O_2 solution in H_2O, Acros Organics, 35 wt %, stabilized p.a.), both in a molar ratio of 2:1 against Ti(IV), and water (25:1 H_2O:Ti(IV) molar ratio) were added to the wet titanium hydroxide precipitate. The mixture was refluxed in air at ∼80 °C for 2 h. A clear, red-colored citrato-peroxo precursor solution of Ti(IV) was thus obtained with a metal ion concentration of ∼0.86 M.

Lead(II) and calcium(II) citrate precursors were added to the former Ti(IV) solution at room temperature to obtain a transparent $(Pb_{1-x}Ca_x)TiO_3$ precursor solution with the desired nominal composition. Commercially available calcium citrate tetrahydrate ($Ca_3(O_2CCH_2C(OH)(CO_2)CH_2CO_2)_2{\cdot}4H_2O$, Aldrich, 99%) was used as the calcium reagent. In the case of the lead citrate reagent, this compound was obtained through the reaction of lead acetate(II) trihydrate ($Pb(OCOCH_3)_2{\cdot}3H_2O$, Aldrich, 99%) with citric acid. Both reagents were dissolved at room temperature in a flask with plentiful deionized water in a 1:2 lead acetate: citric acid molar ratio. The resulting reaction mixture was stirred for 5 min and settled for 15 min. The precipitated lead compound was filtered, washed, and dried in a furnace at 60 °C for 24 h. The empirical formula of the lead(II) citrate reagent thus synthesized corresponds to $Pb(C_6H_6O_7)H_2O$.[33]

As summarized in Figure 1, aqueous solutions with nominal compositions of $(Pb_{0.76}Ca_{0.24})TiO_3$ and $(Pb_{0.50}Ca_{0.50})TiO_3$ (hereinafter denoted as PCT24 and PCT50, respectively) were synthesized containing a 10 mol % excess of Pb^{2+}. The pH of these solutions was adjusted to ∼8.5 by the addition of ammonia (NH_3 solution in H_2O, Merck, 32 wt %) and/or monoethanolamine ($H_2NCH_2CH_2OH$, Aldrich, 99.5+%), because lower pH values lead to the precipitation of lead citrate.[33] A volume of additional water, up to a 65:1 water:Ti(IV) molar ratio, was necessarily added to the PCT50 solutions to obtain a transparent and precipitate-free solution. Aqueous PCT24 and PCT50 stock solutions with a concentration of ∼0.35 and ∼0.25 M (referred as the equivalent molarity of PCT) were thus obtained. Aliquots of the former solutions were dried on Petri dishes in a furnace at 60 °C for 24 h, obtaining transparent and glassy gels.

For the preparation of the films, stock solutions were diluted with distilled water (PCT24 solution) or concentrated by water evaporation (PCT50 solution) to a concentration of ∼0.30 M. Previous to the film deposition, these solutions were refluxed at 100 °C for 1 h to decompose the excess H_2O_2.

2.2. Thin Films. $Pt/TiO_x/SiO_2/Si$ substrates were used for the deposition of the films. These substrates were previously subjected to a wet chemical treatment[12] in order to improve their wetting by the aqueous solutions.

Films from the PCT24 and PCT50 aqueous solutions with a concentration of ∼0.3 M were deposited onto these substrates by spin-coating at 3000 rpm for 30 s. Each film comprised 4 layers. The as-deposited layers were successively dried and pyrolyzed for 2 min on each of three hot plates stabilized at temperatures of 200, 300, and 450 °C. The crystallization of the layers was carried out by rapid thermal processing (RTP) in air at 650 °C for 50 s, with a heating rate of ∼30 °C/s. A total of 4 layers was successively deposited, dried, pyrolyzed, and crystallized. The last deposited layer was treated by RTP at 650 °C, but for a time of 1 h.

2.3. Characterization Techniques. The thermal decomposition mechanism of the PCT gels was studied by means of thermogravimetric analysis (TGA 951−2000, TA instruments) coupled on-line to a Fourier transform infrared spectrometer (Bruker IFS 48) or to a quadrupole mass spectrometer[34] (Thermolab VG Fisons), working in the temperature range of 25−750 °C with a heating rate of 10 °C/min in a dry air flow rate of 100 mL/min. Both complementary techniques (TGA−FTIR and TGA−MS) allowed us to determine the nature of the evolved gases emitted during the thermal decomposition of the gels. In the TGA−MS analysis, the ionization energy was set to 20 eV in order to avoid the fragmentation of H_2O ($m/z = 18$) into OH ($m/z = 17$), which would interfere with the signal of NH_3 ($m/z = 17$).[32] Ions with m/z values between 15 and 115 were collected by this technique, whereas infrared vibrations in the range of 4000−400 cm^{-1} were detected by TGA−FTIR.

X-ray diffraction with grazing incidence (GIXRD) geometry was carried out to study the structure of the crystalline films, using a powder Siemens D500 diffractometer with a Cu anode. A 0.4° Soller slit and a LiF monochromator were used for the GIXRD analysis, with a grazing incidence angle of 2°.

The microstructure of the film surface was observed by scanning electron microscopy (JSM 6335F NT) with an acceleration voltage of 10 kV working under field emission conditions (FEG-SEM). Cross-section images of the films were also obtained and their average thickness was calculated from these images.

Using a shadow mask, top dot Pt electrodes of 50 nm thickness and ∼0.2 mm^2 surface area were deposited on the film surfaces using a sputter instrument (BAL-TEC SCD 050) working at 80 mA for 300 s. The capacitors thus obtained were subsequently RTP annealed in oxygen at 500 °C for 10 min. Dielectric and ferroelectric characterization of the films was performed by parallel plate capacitor-type electrical measurements. The variation of the dielectric constant (k') with temperature at various frequencies was measured for the PCT films with a LCR-meter HP 4284A instrument working with an amplitude signal of 10 mV. Leakage

(32) Hardy, A.; Van Werde, K.; Vanhoyland, G.; Van Bael, M. K.; Mullens, J.; Van Poucke, L. C. *Thermochim. Acta* **2003**, *397* (1−2), 143.
(33) Kourgiantakis, M.; Matzapetakis, M.; Raptopoulou, C. P.; Terzis, A.; Salifoglou, A. *Inorg. Chim. Acta* **2000**, *297*, 134.
(34) Mullens, J. EGA−Evolved Gas Analysis. In *Handbook of Thermal Analysis and Calorimetry*; Gallagher, P. K.; Brown, M. E., Eds.; Elsevier Science: Amsterdam, 1998; Vol. 1: Principles and Practice.

Table 1. Physicochemical Properties of the Aqueous PCT Precursor Solutions

composition	reagents and solvents	molar ratios	physicochemical characteristics[a]	solution aging: with time	solution aging: with temp (60 °C)
$(Pb_{0.76}Ca_{0.24})TiO_3$ (PCT24)	$HOOCCH_2C(OH)(COOH)CH_2COOH$ H_2O_2, H_2O, NH_3 $Ti(OCH(CH_3)_2)_4$, $Pb(C_6H_6O_7)_2{\cdot}H_2O$ $Ca_3(O_2CCH_2C(OH)(CO_2)CH_2CO_2)_2{\cdot}4H_2O$	citric acid:Ti(IV) 2:1, H_2O_2:Ti(IV) 2:1, H_2O:Ti(IV) 25:1	∼0.35 M, ∼1 mg/L, ∼8.5	stable solution (up to a year)	gelation (24 h), transparent gel; gelation (>24 h), transparent gel
$(Pb_{0.50}Ca_{0.50})TiO_3$ (PCT50)	$HOOCCH_2C(OH)(COOH)CH_2COOH$ H_2O_2, H_2O, NH_3 $Ti(OCH(CH_3)_2)_4$, $Pb(C_6H_6O_7)\cdot H_2O$ $Ca_3(O_2CCH_2C(OH)(CO_2)CH_2CO_2)_2{\cdot}4H_2O$	citric acid:Ti(IV) 2:1, H_2O_2:Ti(IV) 2:1, H_2O:Ti(IV) 90:1	∼0.25 M, ∼1 mg/L, ∼8.5	precipitation of calcium citrate in the solution after 2 weeks	gelation (24 h), tran sparent gel; gelation (>24 h), translucent gel

[a] Values represent concentration (referred to as the equivalent moles of PCT per liter of solution), density, and pH, respectively.

current densities were also measured in the films by the step relaxation technique[35] using a Keithley 6512 electrometer and a HP 3325A pulse generator. Ferroelectric hysteresis loops were obtained in the films by means of a modified Sawyer−Tower circuit using a HP 8116A pulse generator of sinusoidal waves with 1 kHz frequency and an amplitude of 3.5 V.

3. Results

The main physicochemical properties of the PCT24 and PCT50 solutions prepared by the aqueous solution−gel method are summarized in Table 1. Both solutions were stored at room conditions in simple glassware. However, the PCT50 solution was stable for only a few weeks, whereafter a precipitate was formed. The supernatant was decanted and the precipitate was dried (80 °C/24 h) and subjected to X-ray diffraction; we observed that it is mainly formed by crystalline calcium citrate. On the other hand, the PCT24 solution remained stable even up to a year, and neither gelation (sol−gel transition) nor precipitation was observed. Concerning the sol−gel transition with temperature, the formation of transparent glassy gels was observed for both solutions after a treatment of 24 h at 60 °C in an open container. If longer heating times were applied, the PCT50 system changes from a transparent to a translucent gel.

Figure 2 shows the TGA and the corresponding derivative (DTG) curves measured during the thermal treatment of the PCT24 and PCT50 aqueous gels (panels a and b of Figure 2, respectively). Five steps can be distinguished in the thermal decomposition of both gels, centered at temperatures of ∼75, ∼210, ∼345, ∼460, and ∼540 °C (PCT24) or 605 °C (PCT50). Respective associated weight losses with these steps are ∼2.8, ∼26.4, ∼16.9, ∼19.6, and ∼1.5 wt % for the PCT24 gel and ∼2.9, ∼33.7, ∼14.4, ∼20.7, and ∼1.9 wt % for the PCT50 gel. Attending to the DTG data, the broad peak attributed to the second step (210 °C) indicates that various overlapping processes may occur at this temperature interval. On the contrary, a more homogeneous decomposition process is found during the fourth step, which results in the sharp peak observed at 460 °C. Regarding the last step of the decomposition process of both gels, the temperature at which it is developed differs as a function of the PCT composition (540 °C for the PCT24 gel and 605 °C for the PCT50 gel).

Analysis of the evolved gases emitted during the decomposition of the gels was carried out by means of on-line coupled FTIR and MS techniques. The most representative IR bands and mass fragments analyzed, together with the temperatures at which the corresponding peaks were detected, are summarized in Table 2.

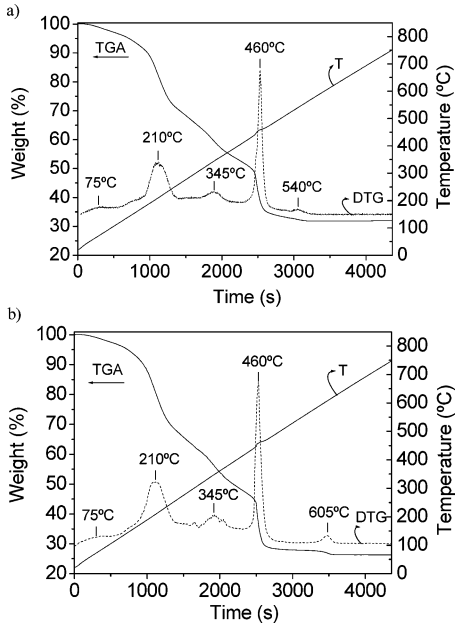

Figure 2. TGA−DTG curves of the (a) PCT24 and (b) PCT50 gels.

Figure 3 shows the evolution with time of some characteristic IR bands analyzed during the TGA−FTIR analysis of the PCT24 (Figure 3a) and PCT50 (Figure 3d) gels. These are 940−913 cm^{-1} ($\delta(NH_3)$ of ammonia, NH_3), 2217−2137 cm^{-1} (ν(C═O) of carbon monoxide, CO), and 2268−2395 cm^{-1} (ν(C═O) of carbon dioxide, CO_2). Furthermore, the total amount of the evolved gases collected in the spectrum range of 400−4000 cm^{-1} as a function of time is also depicted (total integrated signal). The evolution with time of certain ions fragments as a function of their mass/charge ratio (m/z) is also shown in this figure (panels b and c of Figure 3 for the PCT24 gel and panels e and f of Figure 3 for the PCT50 gel). Thus, m/z values of 17, 18, 30, and 44 correspond to fragments of NH_3^+, H_2O^+, NO^+, and CO_2^+, respectively. Citric acid and its intermediates produce ions with m/z values of 39 ($C_3H_3^+$), 40 ($C_3H_4^+$), 41 ($^{13}C_3H_4^+$), 68 ($C_4H_4O^+$), and 112 ($C_5H_4O_3^+$).[32] In panels c and f of Figure 3, the fragments of citric acid are represented by m/z values of 41 and 68.

Below 140 °C, a slight peak in the TGA−MS curve of the water signal ($m/z = 18$) can be discerned in the PCT24

(35) Waser, R.; Klee, M. *Integr. Ferroelectr.* **1992**, *2*, 23.

Table 2. TGA and EGA Data of the Aqueous Solutions derived PCT Gels

	weight loss (%)		peak T (° C)					
T interval (° C)	PCT24	PCT50	PCT24	PCT50	TGA−FTIR bands (cm^{-1})	TGA−MS (m/z)	fragment	processes
					Step 1			
<105	∼2.8	∼2.9	∼105	∼105		18	H_2O	*evaporation of residual solvent*
					Step 2			
140−250	∼26.4	∼33.7	∼210	∼205	940−913	17	NH_3	*decomposition of organic constituents of the gel*
			∼205	∼205		41	$^{13}C_3H_4$	ammonium citrate → citric acid + NH_3
			∼225	∼225		18	H_2O	citric acid → aconitic acid + H_2O
			∼225	∼225		68	C_4H_4O	aconitic acid → itaconic acid + CO_2
			∼230	∼240	2268−2395	44	CO_2	
					Step 3			
250−400	∼16.9	∼14.4	∼300	∼310		41	C_2H_3N	*decomposition/combustion of organics bonded to the metal ions (citrateperoxo ligands)*
			∼300, ∼355	∼310, ∼370		41	$^{13}C_3H_4$	amides[a] → C_2H_3N
			∼345	∼355		18	H_2O	$C_xH_yO_z$ → CO + CO_2 + H_2O + CO_3^{2-} [b]
			∼350	∼365	2268−2395	44	CO_2	$Ca^{2+} + CO_3^{2-}$ → $CaCO_3$
			∼375	∼375	2217−2137		CO	
					Step 4			
400−500	∼19.6	∼20.7	∼450	∼460		41	$^{13}C_3H_4$	*decomposition/combustion of remanent organics*
			∼455	∼465	940−913	17	NH_3	amides → NH_3, NO
			∼455	∼465, ∼500		30	NO	$C_xH_yO_z$ → CO + CO_2 + H_2O
			∼455	∼465	2268−2395	44	CO_2	
			∼455	∼465		18	H_2O	
			∼455	∼465	2217−2137		CO	
					Step 5			
>500	∼1.5	∼1.9	∼540	∼620		44	CO_2	*decomposition of calcium carbonate* $CaCO_3$ → CaO + CO_2

[a] From the reaction of NH_3 with carboxylate groups (e.g., aconitic/itaconic acid). [b] From the pyrolysis of calcium citrate.

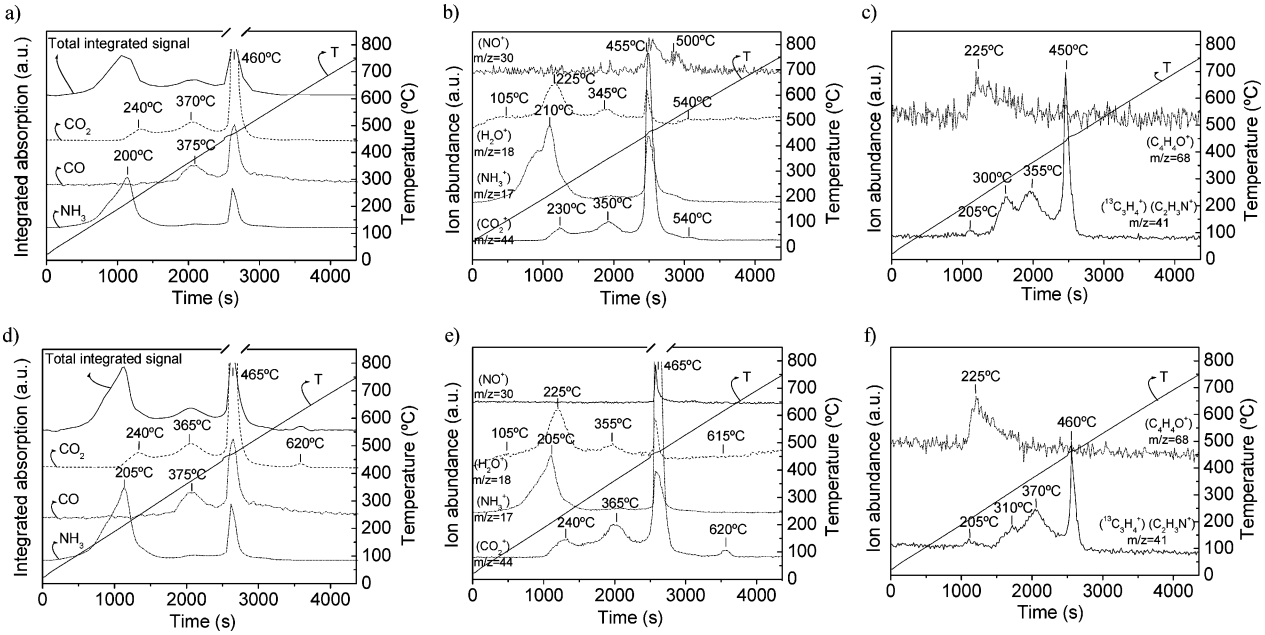

Figure 3. TGA−FTIR analysis of the (a) PCT24 and (d) PCT50 gels. TGA−MS analysis of the (b,c) PCT24 and (e,f) PCT50 gels.

and PCT50 gels (panels b and e of Figure 3). Similar weight losses of ∼2.8 and ∼2.9 wt % are associated with this process in the TGA curves of both gels (Figure 2). In the temperature range between 140 and 250 °C, several processes are developed that lead to the largest weight loss measured in the TGA curves of the PCT24 and PCT50 gels (∼26.4 and ∼33.7 wt %, respectively). At 205−210 °C, the first peak of ammonia can be observed in both TGA−FTIR and TGA−MS of the gels. This signal corresponds to the decomposition of ammonium citrate, formed from the ammonia and the excess of citric acid present in the Ti(IV) solution. In the 205−225 °C interval, peaks ascribed to water ($m/z = 18$) and ion fragments of 41 ($^{13}C_3H_4^+$) and 68 ($C_4H_4O^+$), corresponding to fragments derived from decomposition of citric acid,[36] can be observed in the TGA−

(36) Van Werde, K.; Mondelaers, D.; Vanhoyland, G.; Nelis, D.; Van Bael, M. Mullens, K. J.; Van Poucke, L. C. *J. Mater. Sci.* **2002**, *37*, 81.

MS graphs of both gels. This decomposition occurs as follows

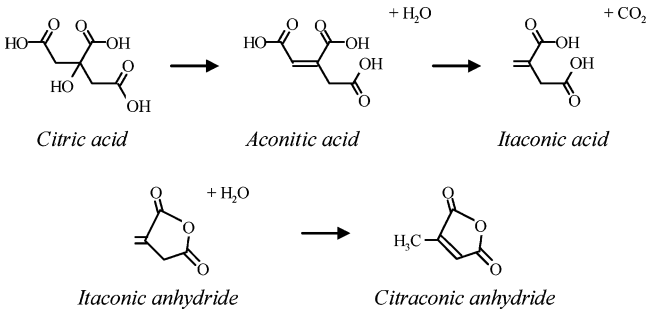

The dehydration of citric acid into aconitic acid with the subsequent evolution of a molecule of water occurs at this temperature (205−225 °C). The subsequent decarboxylation of aconitic acid into itaconic acid is observed at 230−240 °C, where the first peak in the profile of CO_2 is detected in both TGA−FTIR and TGA−MS graphs of the gels. Note that the maximum of this peak does not match with that associated with the elimination of water at ∼225 °C, which is indicative that a decarboxylation indeed occurs instead of a combustion. Itaconic acid can react further to form the cyclic itaconic anhydride and/or citraconic anhydride, as shown above. However, amides can also be formed by the nucleophilic reaction of NH_3 with carboxylate groups (e.g., itaconic acid), finally leading to the formation of nitriles.[32] This could explain the peak of $m/z = 41$ at 300−310 °C that might be ascribed to $C_2H_3N^+$ (panels c and f of Figure 3). Organic compounds in the sample are eliminated further during the third step of the decomposition pathway of the PCT24 and PCT50 gels, around ∼345 °C. The simultaneous evolution of water and CO_2, observed in both TGA−FTIR and TGA−MS analyses, is ascribed to the combustion of organics. At ∼460 °C, combustion of residual species takes place with a large amount of oxygen consumed (the signal at $m/z = 32$ (O_2^+) reveals a strong decrease below the background level in the TGA−MS curve, not shown). This leads to the formation of volatile species such as NH_3, NO, and CO (panels b and e of Figure 3) in this step. Finally, during the last step, a weak peak can be discerned in the DTG curves of the PCT24 and PCT50 gels at ∼540 and ∼605 °C, respectively, with small associated weight losses of ∼1.5 and ∼1.9 wt %, respectively. The small $m/z = 44$ signal observed in the TGA−MS analysis (panels b and e of Figure 3) at this temperature indicates that CO_2 is released during this process.

Figure 4 shows GIXRD patterns of the PCT24 and PCT50 crystalline films. All of the peaks could be indexed according to the perovskite crystalline phase. No crystalline secondary phases, at least none greater than 1 wt %, can be observed in the diffractograms, thus indicating the presence of a single perovskite phase under X-ray diffraction.

The micrographs of the films surfaces obtained by FEG−SEM (Figure 5) show a homogeneous microstructure in both films. The microstructure consists of spherical grains with an average grain size of ∼100 and ∼50 nm for the PCT24 and PCT50 films, respectively. Thicknesses of ∼240 and ∼250 nm for the PCT24 and PCT50 films, respectively, were

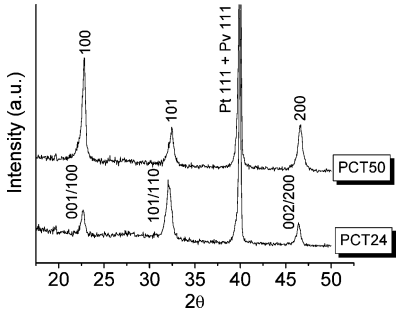

Figure 4. GIXRD patterns of the PCT24 and PCT50 films (Pv, perovskite; Pt, platinum).

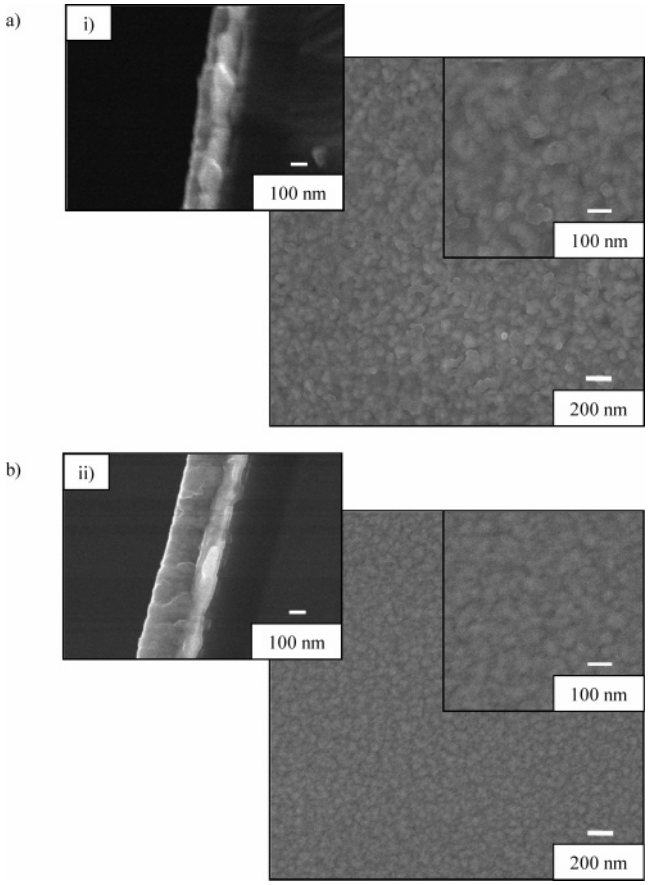

Figure 5. SEM micrographs of the (a) PCT24 and (b) PCT50 films (plan-view). Insets show cross-section images of the (i) PCT24 and (ii) PCT50 films.

calculated from the cross-section images shown in the insets of this figure. An estimated error of ∼5% nm should be taken into account in these values (thicknesses measured by profilometry, ∼245 nm for both films, are within this experimental error).

Figure 6 shows the variation of the dielectric constant (k') with temperature of the PCT24 and PCT50 films measured at various frequencies. Insets in the figure correspond to the variation of the loss tangent (tan δ) with temperature. It should be noticed that permittivity values are subjected to a slight fluctuation (∼10%) according to the experimental error introduced by the thickness and top electrode surface area calculations. A characteristic ferroparaelectric transition can be observed in the PCT24 film (Figure 6a) with values of the dielectric constant of 1350 at T_m (temperature at which k' is maximum, 340 °C) and 920 at room temperature,

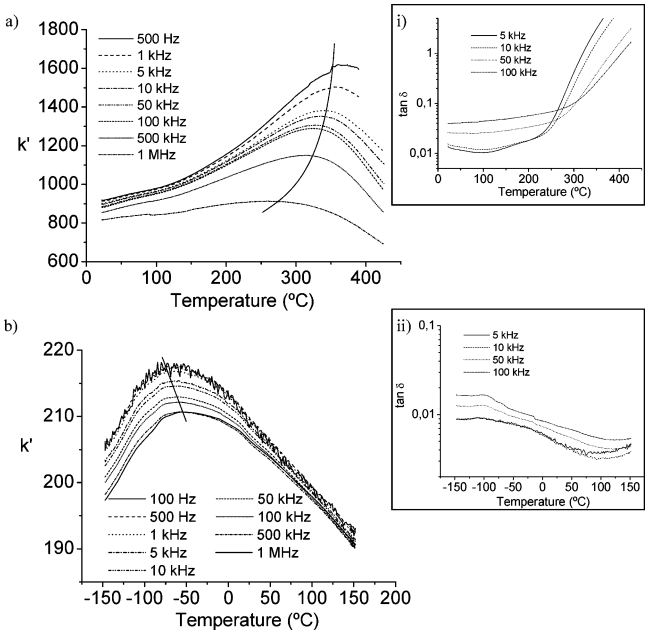

Figure 6. Variation of the dielectric constant (k') with temperature of the (a) PCT24 and (b) PCT50 films, measured at various frequencies. Continuous lines are depicted as a guide for the eye for the temperature maximum shift. Insets show the variation of the loss tangent (tan δ) with temperature for the (i) PCT24 and (ii) PCT50 films.

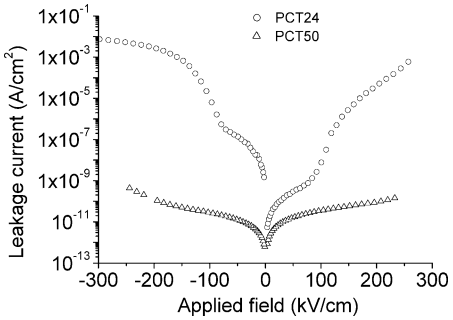

Figure 7. Field dependence of leakage currents for the PCT24 and PCT50 films.

measured at 10 kHz. A displacement of the dielectric constant maxima toward lower temperatures as the measuring frequency increases is also observed in this figure (see solid line). In the case of the PCT50 composition, a clear relaxor-like ferroelectric behavior is observed in Figure 6b. Note how the temperature of the maximum of the dielectric constant shifts to higher values when the frequency increases, which is characteristic of relaxor materials. A diffuse ferro-paraelectric transition around −55 °C (T_m) is observed from data measured at 10 kHz, with an associated k' value of 215. At room temperature, this value slightly decreases to 205. Both PCT24 and PCT50 films show low values of tan δ at room temperature and 10 kHz (0.015 and 0.005, respectively), as observed from the respective insets of this figure.

Figure 7 shows the field dependence dc leakage currents of the PCT films at room temperature. Large and asymmetric leakage currents are observed for the PCT24 film. However, this effect is not observed in the PCT50 film, and a low leakage current density is obtained here (values below 1×10^{-9} A/cm^2).

The ferroelectric character of the PCT24 film was analyzed by the ferroelectric hysteresis loop of Figure 8. No analysis

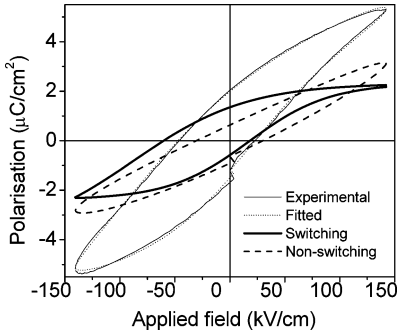

Figure 8. Ferroelectric hysteresis loop of the PCT24 film. The nonswitching contribution to ferroelectric domains is also depicted.

was carried out on the PCT50 film, because this perovskite composition shows a relaxor-ferroelectric behavior (shown above for these films) with a low ferroelectric response.[27] A slanted, asymmetric, low-remanent P(E) loop was obtained for the PCT24 film. Values of remanent polarization (P_r) of ∼1.0 μC/cm^2 and coercive field (E_c) of ∼40 kV/cm were measured at a maximum amplitude of 3.5 V. Larger voltage bias could not be applied in the measurement because high leakage conduction resulted in the film, thus preventing us from obtaining larger polarization values. The asymmetry of the loop is corroborated by the high bias displacement obtained (−20 kV/cm). The nonswitching contribution to this ferroelectric hysteresis loop is also displayed in this figure.

4. Discussion

Air-stable and precipitate-free stock solutions of calcium-modified lead titanate, $(Pb_{1-x}Ca_x)TiO_3$, with Ca^{2+} contents of 24 and 50 at. % ($x = 0.24$ and 0.50) were obtained by the aqueous solution−gel method here reported. The properties of these solutions differ depending on their respective compositions (PCT24 or PCT50). Although both solutions were obtained by the same synthesis route (Figure 1), a larger amount of water had to be added to the PCT50 system in order to obtain a clear and transparent solution (see Table 1). The reason lies in the low solubility that the calcium citrate reagent exhibits in the aqueous media (solubility of 0.9 g/L at room temperature for pH levels above 4.5). This fact strongly influences the stability of the PCT50 precursor solutions obtained, because precipitation of calcium citrate in this solution leads to a short-term aging (2 weeks), whereas the PCT24 solution remains stable with time (more than a year). This effect is also observed when studying the gelation behavior of these solutions with temperature, because the glassy and transparent gels obtained from the PCT50 solution (60 °C/24 h) become translucent once the amount of solvent evaporated has reached a certain critical value (longer aging times at 60 °C, see Table 1), that is, the supersaturation of the solution. Among the different calcium reagents tested in the literature for the synthesis of $(Pb_{1-x}Ca_x)TiO_3$ solutions,[28] the incorporation of Ca^{2+} contents over 40 at. % ($x > 0.4$) was achieved only by the use of calcium acetate.[27] With the aqueous solution−gel method, successful partial substitutions of Pb^{2+} by Ca^{2+} up to 50 at. % in the PCT system have been carried out using calcium citrate as the Ca^{2+} precursor.

The thermal decomposition of both PCT24 and PCT50 gels is carried out through a five-step mechanism (Table 2).

Below 140 °C, the evaporation of residual water still present within the gel network takes place. Organic constituents of the gel are decomposed during the second step at temperatures between 140 and 250 °C. The decomposition of the ammonia and nonmetal coordinated citrates begins here. During the third step (250−400 °C), the combustion of the citrate and peroxo ligands bonded to the metal ions in the PCT gel takes place. Furthermore, the decomposition of the amides formed during the former step also happens here. Further elimination of residual organics occurs during the fourth step at temperatures between 400 and 500 °C. Finally, the small weight losses observed above 500 °C (fifth step) associated with the CO_2 evolution are attributed to the decomposition of calcium carbonate ($CaCO_3$), formed in the previous steps from the pyrolysis of calcium citrate.[37] The difference in the temperature at which this decomposition is produced in both PCT gels could be related to the different nature of the respective carbonates formed (purity, polymorphism/allotropy, etc). As the concentration of Ca^{2+} in the $(Pb_{1-x}Ca_x)TiO_3$ composition of the gel is bigger, the amount of $CaCO_3$ formed is therefore larger, which explains the larger weight loss detected in the PCT50 gel at these temperatures compared to the PCT24 gel. The elucidation of the thermal decomposition pathway of the PCT gels and the understanding of the different processes that are carried out during the thermal treatment allowed us to establish the optimum temperatures at which the as-deposited films must be treated: 200, 300, and 450 °C for the drying and pyrolysis of the films and 650 °C for their crystallization.

In this way, single perovskite films were obtained at 650 °C (Figure 4). The PCT24 films show a pseudocubic structure, where the characteristic doublets of the tetragonal structure observed in the counterpart bulk ceramics[38] are here overlapped (001/100, 101/110, and 002/200). This is because of the development of stresses in the material produced during the film processing.[39] For the PCT50 film, the perovskite reflections should be adjusted to an orthorhombic structure that has been previously observed by neutron diffraction on ceramic powders of the same composition.[40] Differences in the grain size as a function of the composition of the PCT crystalline film are deduced from the surface micrographs of Figure 5 (∼100 and ∼50 nm for the PCT24 and PCT50 film, respectively). The influence of the Ca^{2+} content in the PCT composition on the nucleation and crystal growth of films obtained by RTP has been previously reported for PCT films prepared with other sol−gel methods,[41] obtaining a trend similar to that shown here. This indicates that grain size of these films is mainly related to the Ca^{2+} content of the PCT composition rather than to the solution process followed.

From the electrical data obtained, the potential applications of the PCT films obtained through the aqueous solution−gel method in the technology of functional microelectronic devices are evaluated. In the PCT24 film, the displacement of the dielectric constant maxima toward lower temperatures upon increasing the measuring frequency (Figure 6a) can be observed, similar to that expected for the polar domain relaxation but at rather low frequencies.[42] The appearance of this relaxation could be related to the presence of extrinsic defects in the film (e.g., low-quality interfaces) that yield an increase in the series resistance of the sample producing the observed effect. Despite this, acceptable values of the dielectric constant and loss tangent were measured in the PCT24 films. The dielectric constant values of these films are similar to those obtained in films with the same composition (PCT24) prepared by other sol−gel methods.[43] However, the low difference between the dielectric constant at T_m and that at room temperature (∼1350 and ∼920 respectively, at 10 kHz) is an indication of the low content of switchable ferroelectric phase in the film and the larger presence of nonswitchable phase (porosity, grain boundaries, etc.) dispersed in the bulk film.

High leakage currents are measured in the PCT24 film (Figure 7) that suppose an important drawback for the integration of these films into microelectronic devices. Furthermore, he strong asymmetry of these data denotes the difference in the nature of top/bottom electrode junctions in this film. The experimental setup of the leakage current density measurements indicates that leakages are higher at the top electrode, which could be an indication of roughness at the top surface of the film.[44] But leakages are also quite high at the film-bottom electrode junction, indicating the presence of a defective layer here as well. These detrimental interfaces formed in the heterostructure of the PCT24 film would be responsible of the dielectric relaxation discussed above (Figure 6a). Both asymmetry and large values of the leakage current densities of the PCT24 film prevent the correct polarization of the film, leading lower values than those that would be obtained if the film could be better polarized (Figure 8). Values of P_r near 20 $\mu C/cm^2$ have been reported for PCT24 films prepared by other sol−gel methods.[45] Here, the aqueous-derived PCT24 film showed a low remanent polarization value that at first sight discourages its application in ferroelectric devices.

On the other hand, the relaxorlike behavior observed in the PCT50 film (Figure 6b), with the relatively high k' values (205−210) compared with those of other high k single oxides[46] and the low tan δ (0.005) measured at room temperature, shows the viability of this material for applications in DRAMs[47] and high-frequency components (con-

(37) Calzada, M. L.; Malic, B.; Sirera, R.; Kosec, M. *J. Sol−Gel Sci. Technol.* **2002**, *23*, 221.
(38) Mendiola, J.; Alemany, C.; Jiménez, R. E. Maurer; Calzada, M. L. *Bol. Soc. Esp. Ceram. Vidreo* **2004**, *43* (3), 620.
(39) Mendiola, J.; Calzada, M. L.; Ramos, P.; Martín, M. J.; Agulló-Rueda, F. *Thin Solid Films* **1998**, *315* (1−2), 195.
(40) Ranjan, R.; Singh, N.; Pandey, D.; Siruguri, V.; Krishna, P. S. R.; Paranjpe, S. K.; Banerjee, A. *Appl. Phys. Lett.* **1997**, *70* (24), 3221.
(41) Bretos, I.; Ricote, J.; Jiménez, R.; Mendiola, J.; Jiménez Riobóo, R. J.; Calzada, M. L. *J. Eur. Ceram. Soc.* **2005**, *25*, 2325.
(42) Mitsui, T.; Tatsuzaki I.; Nakamura, E. *Ferroelectricity and Related Phenomena*; Gordon and Breach: London, 1976; Vol. 1: An Introduction to Physics.
(43) Sirera, R.; Calzada, M. L.; Carmona, F.; Jiménez, B. *J. Mater. Sci. Lett.* **1994**, *13* (24), 1804.
(44) Zhao, Y. P.; Wang, G. C.; Lu, T. M. *Phys. Rev. B* **1999**, *60* (12), 9157.
(45) Calzada, M. L.; Jiménez, R.; Ramos, P.; Martín, M. J.; Mendiola, J. *J. Phys. IV* **1998**, *8*, 53.
(46) Boyd, I. W.; Zhang, J. Y. *Solid-State Electron.* **2001**, *45*, 1413.
(47) Auciello, O.; Scott, F.; Ramesh, R. *Phys. Today* **1998**, *51* (7), 22.

sumer portable communications and radar systems). Furthermore, the low leakage current densities measured ($<1 \times 10^{-9}$ A/cm^2) would prevent the thermal breakdown of the film when the capacitor is successively charge-injected/released (refreshed), making the role of the system not only feasible but also effective.[48]

Conclusions

Air-stable and precipitate-free solutions with compositions of $(Pb_{0.76}Ca_{0.24})TiO_3$ (PCT24) and $(Pb_{0.50}Ca_{0.50})TiO_3$ (PCT50) have been synthesized by an entirely aqueous solution−gel route. However, the stability of the precursor solutions strongly decreases when large amounts of calcium citrate have to be incorporated to the solution.

The hydrophilicity of the platinized substrates and hence their wetting by the aqueous solutions is improved by a chemical treatment of cleaning that allows the thin film preparation. Thus, crystalline films with a single perovskite structure can be obtained after RTP treatment at 650 °C. The PCT50 films develop microstructures formed by grains smaller than those of the PCT24 films. A clear relaxor-ferroelectric character with a diffuse ferroparaelectric transition and a high dielectric constant at room temperature is obtained for the PCT50 films. Both characteristics, together with the low leakage currents measured (below 10^{-9} A/cm^2), indicate the suitability of this composition for its potential use in DRAMs and high-frequency components. The PCT24 films present a low polarization value ($\sim$1.0 μC/cm^2) and high leakage current densities that suppose critical drawbacks for their application in ferroelectric devices. Further investigations are in progress to improve the electrical properties of these films.

Acknowledgment. This work has been supported by the Spanish Project CICyT MAT2004-02014. I.B. thanks to the Spanish MEC for his Ph.D. FPI grant and for the financial support for his short-term stay at a foreign laboratory. A.H. and M.K.V.B. are postdoctoral fellows of the Research Foundation Flanders (F.W.O.−Vlaanderen).

CM061767E

(48) Scott, J. F. *Ferroelectric Memories*; Springer: Heidelberg, Germany, 2000.